Sensors and Materials, Vol. 11, No. 6 (1999) 369–382
MYU Tokyo

S & M 0380

Fabrication of a Sensitive Germanium Microbolometer for Tympanic Thermometry

Chung-Nan Chen and Jin-Shown Shie

Institute of Electro-Optical Engineering, National Chiao Tung University
1001 Ta Hsueh Road, Hsinchu, Taiwan

(Received August 10, 1999; accepted August 10, 1999)

Key words: Ge thin film, microbolometer, noise, detectivity

Fabrication of a complementary-metal-oxide-semiconductor (CMOS)-process-compatible microbolometer for tympanic thermometry using an amorphous germanium thin film as the temperature-sensitive element has been studied. Heat treatment of the deposited films, with or without passivation, at different annealing temperatures was investigated for optimizing the sensitivity of the material and for considering the compatibility of the CMOS process. Microbolometers structured with a thermally isolated membrane to enhance the thermal responsivity were fabricated by micromachining. The fabricated devices were characterized by conducting appropriate experiments and evaluated for the necessary thermal and electrical parameters useful in applications. It has been found that, for an annealing condition around 370°C for two hours, the passivated floating Ge thermistor has a 3%/°C temperature coefficient of resistance (TCR) and a comparably low flicker noise relative to other conditions. In a vacuum, the passivated device with an area of 250×250 μm^2 shows a responsivity up to 400 kV/W at 1 Hz, and a normalized detectivity D* of 1.2×10^8 and 5.2×10^7 $cmHz^{1/2}/W$ at 3 Hz and 30 Hz, respectively. These measured values also prove that the device, in its current structure, can be used as a sensitive radiation detector for tympanic thermometers.

1. Introduction

The resistive thermal detector for infrared sensing without cryogenic cooling was invented by Langely[1] more than one hundred years ago and was originally named a bolometer. Compared with other members in the family of radiative thermal detectors, bolometers are superior to thermopiles and pyroelectric detectors[2,3] in sensitivity and in simplicity of fabrication, despite their large offset. At present, a bolometer can be fabricated by mature micromachining technology into a focal-plane-array (FPA) structure for high-performance uncooled thermal imaging,[4,5] in which a signal processing circuit is integrated monolithically on a Si substrate.

There are two types of bolometer, the metal-film type and the thermistor type. The latter type usually has a much higher temperature coefficient of resistance (TCR), but this is offset by greater flicker noise. More importantly, most complementary metal oxide semiconductor (CMOS) foundries are reluctant to promise to prepare thermistors other than polysilicon at the moment, because of concerns about worrying potential contamination by nonstandard materials. Research has been focused on finding high TCR materials which are compatible with the standard CMOS fabrication processes in use currently in foundries, so that an integrated microbolometer can be manufactured in small quantities like ASIC, which otherwise would not be acceptable for reasons of cost.

A polysilicon microbolometer has been proposed in reports.[6] It displays excellent TCR at low-doping concentration (3~7%/°C) and is fully compatible with standard IC processes. However, in current submicron CMOS fabrication, the grain size of the polysilicon is in the hundred-angstrom range, which induces abundant trap formations between the grain boundaries; therefore, the flicker noise is inevitably high.[7,8] This prevents polysilicon from being a candidate material for a sensitive bolometer. Replacing polysilicon with low-energy-gap material, such as Si-Ge[9] or Ge,[10–12] is worthy of note. Especially in Ge material, the shallower trap level is expected to induce lower 1/f noise; in addition, contamination of IC equipment is not associated with this material.

Although Ge has long been used in a thermistor bolometer of reasonable high TCR (3~4%/°C), the process-compatibility issue has never been considered in previous reports. In this article, preparation of a thin-film Ge sensor that also addresses the CMOS fabrication process constraints is reported. A highly sensitive micromachined Ge bolometer is fabricated and characterized. Its potential as a thermal radiation detector for tympanic thermometry is also discussed.

2. Experimental

2.1 *Device fabrication*

Thin-film Ge sensors are prepared in two structures, one without passivation and one with an oxide passivation, as shown in Fig. 1 and Fig. 2, respectively.

In Fig. 1, a (100) Si wafer is cleaned and thermally oxidized to obtain a 500 nm field oxide (1a). Then interdigitated electrodes of an e-gun-evaporated titanium thin film are formed by a lift-off process (1b and 1c). Subsequently, high-purity (6N) Ge is used to form

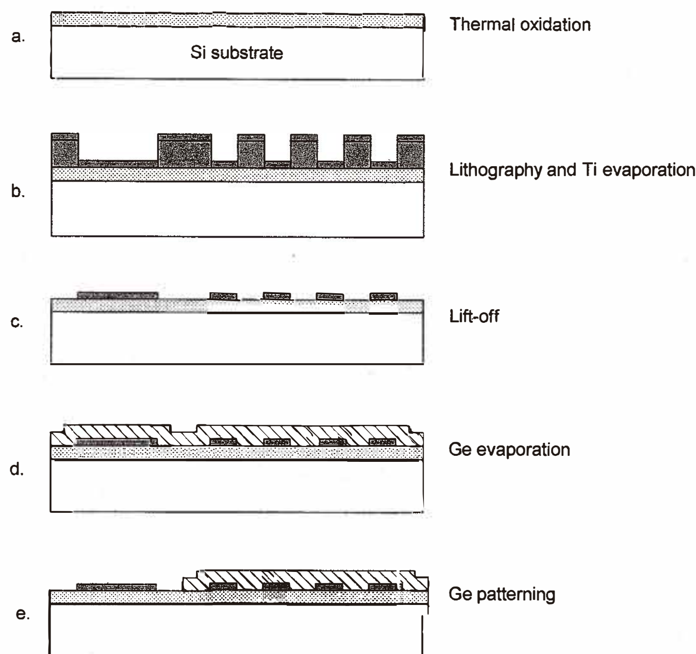

Fig. 1. Preparation of an unpassivated Ge thermistor on a silicon substrate for heat treatment studies.

a thin film of 350 nm on the electrodes by e-gun evaporation under conditions of an electron beam current of 50mA, a deposition rate of 0.2 nm/s and a process pressure of 1×10^{-6} Torr (1d). The film is then subjected to photolithographic etching to define the sensor pattern with an etchant of H_3PO_4: H_2O_2: H_2O= 1: 6: 3 (1e). The finished wafer is sawed into chips for further annealing studies.

In Fig. 2, a 100-nm-thick thermal oxide is first prepared on a (100) wafer, and a 150 nm LPCVD nitride film is added subsequently (2a). Then, as before, the same interdigitated titanium electrodes and Ge film are evaporated, patterned (2b and 2c) and then passivated with 300 nm PECVD oxide (2d). The passivation is opened with contact vias, and aluminum interconnections and bonding pads are formed on the top (2e). A 30 nm NiCr film is sputtered and patterned by a lift-off process to serve as a heat-absorbing black coating (2f). A final lithographic process is used to release the passivation selectively in the area of the etching window (2g). Anisotropic etching by a hydrazine solution (N_2H_4: H_2O= 1: 1) at 90°C is used to create the v-groove cavity beneath the floating membrane whereon the Ge sensor rests (2h). The finished wafers are sawed into dice for heat treatment. Each sample is subjected to the same annealing time of 2 h in nitrogen furnace but at different temperatures.

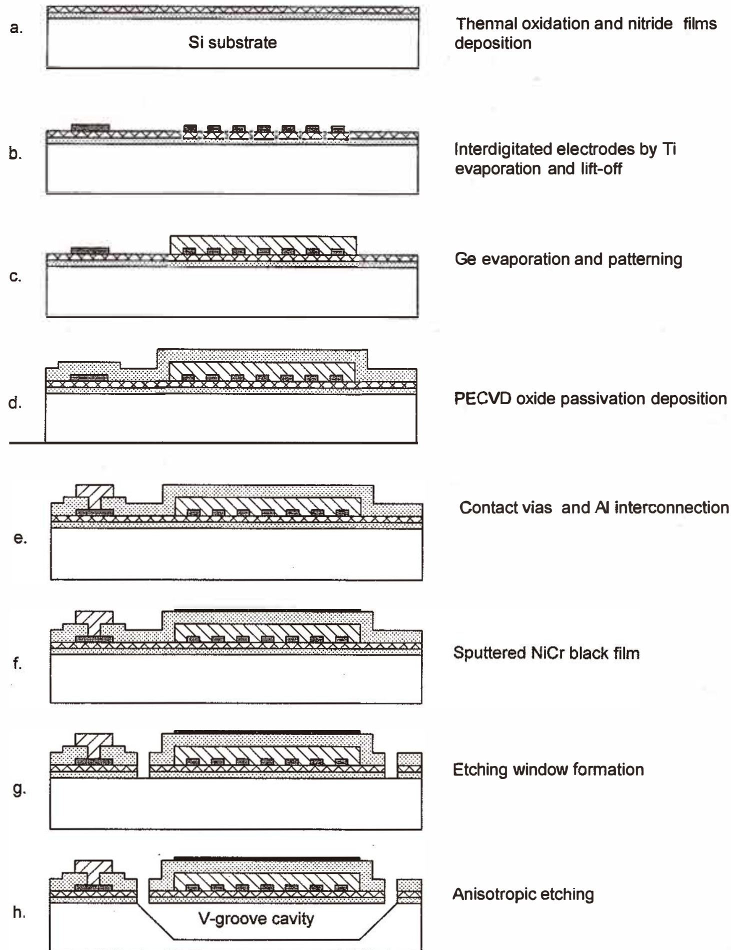

Fig. 2. Preparation of a passivated Ge microbolometer on a (100) silicon substrate. Notice that the Ge film is passivated with 300 nm PECVD oxide, which is a standard process step in a 1.2-μm-CMOS foundry and is used for protecting the Ge film during anisotropic v-groove etching.

The fabricated device, as shown in Fig. 3, has a membrane area of 250×250 μm^2 and a lead structure 170 μm long, 14 μm wide and 0.7 μm thick. The oxide-nitride-oxide (ONO) sandwich structure applied here is well known for reducing the residual stress existing inside the membrane.[13,14]

It must also be emphasized that the device fabrication processes follow what are now provided in CMOS foundries, except in the case of the Ge coating and its annealing, which are possible for the facility to carry out without contamination.

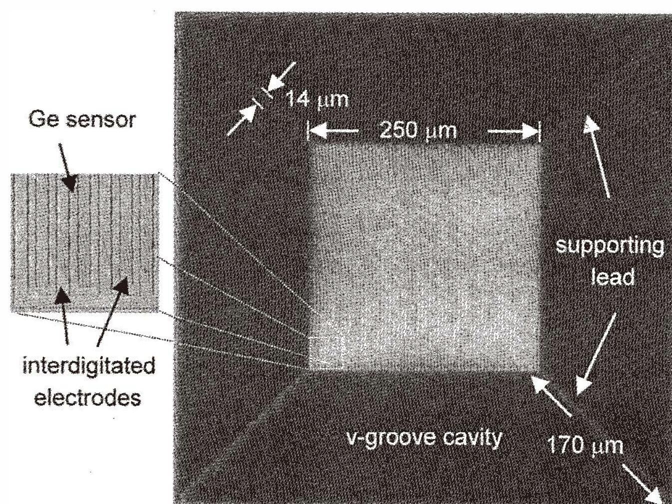

Fig. 3. A photograph of a fabricated Ge microbolometer. The membrane, supported by four leads extending to the substrate, has an area of 250×250 μm^2.

2.2 *Measurements*

All samples were measured for resistance and TCR. The resistivity was calculated according to the geometry of the sensor film. For passivated samples with a complete microbolometer structure, the responsivity and noise were also measured. Figure 4 depicts the measurement setup. A packaged microbolometer is placed on a holder in a chamber that can be evacuated to a designated vacuum pressure. The surrounding wall of the vacuum chamber is water-cooled, so that a constant temperature can be maintained to avoid ambient drift affecting the sensor. The chamber also has a 8–12 μm infrared window to subject the sensor to an external thermal radiation. The radiation is from a calibrated blackbody, which is modulated by a chopper and digitally driven by a PC. The signal from the sensor is read by a lock-in amplifier and processed by a GPIB interface before being recorded by the PC.

For noise measurements, the sensor is shielded and no input of external radiation is allowed.

3. Results and Discussion

Figure 5 shows the measured resistivity and TCR of the Ge films as a function of various annealing temperatures. One notes that both the resistivity and TCR start to drop once the annealing temperature is over 400°C. Since the Ge films were evaporated on cold substrates, an amorphous Ge (α-Ge) state was expected. An α-Ge could induce abundant

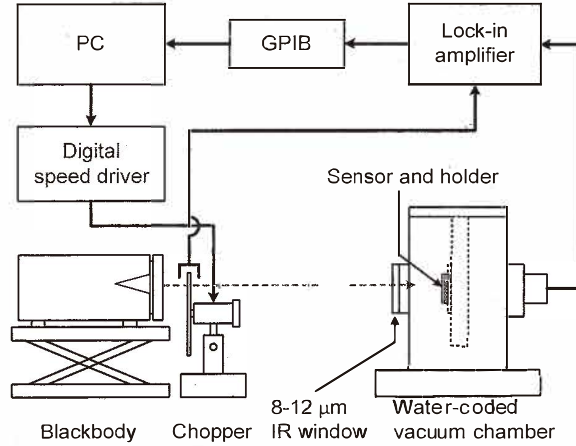

Fig. 4. The experimental setup for characterizations of the Ge microbolometer.

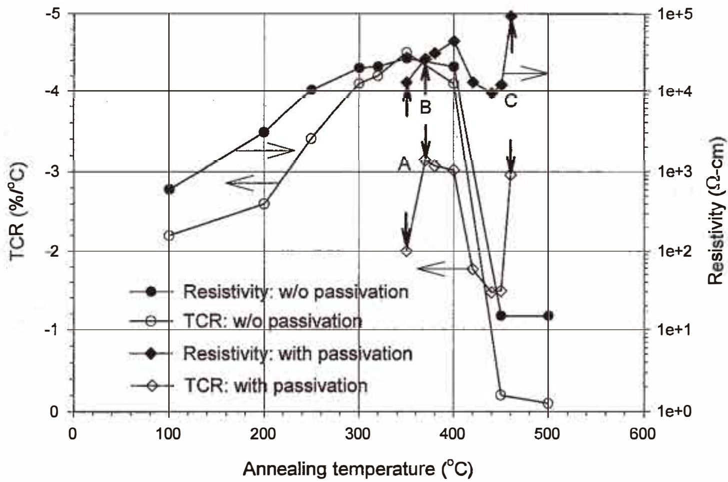

Fig. 5. The resultant TCR and resistivity of the unpassivated (circles) and passivated (diamonds) Ge sensors after various annealing temperatures. Note that the passivated sensors have low TCR and the resistivity variation is not as drastic as in the unpassivated sensors over 400°C.

dangling bonds, thus producing the equivalent amount of trap levels in the energy gap. The traps eliminate free carriers, making the films behave like intrinsic semiconductor and resulting in high resistivity and TCR. High-temperature annealing, possibly around 400°C, initiates recrystallization which induces the crystalline phase.[15] Polycrystalline Ge reduces the density of dangling bonds and the carriers are released to produce higher conductivity in the material. A similar phase transformation occurs for both the passivated and unpassivated samples as indicated in Fig. 5. However, the passivated samples do not show a precipitous drop in resistivity. The interface energy between the Ge film and the passivating oxide might inhibit nucleation to a certain degree. The resistivity and TCR are found to rebound when the annealing temperature is over 450°C. This might be due to the diffusion of the oxygen atoms from PECVD oxide into the Ge film. The atoms create new trapping centers in the sensor films, leading to the increase.

Currently, the actual physics behind the annealed behavior is not yet clear and further material characterizations are required to improve understanding. However, one point is indeed clear from the heat treatment study; for the passivated sensors, the best annealing temperature in reference to the TCR obtained is between 360 to 400°C. This temperature is very beneficial, because all the process steps after the Ge film deposition, including the Al metal annealing, can be performed below 400°C, and these processes do not violate the MOS fabrication constraints.

All the treated films show the Arrhenius behavior in resistance. Figure 6 illustrates the measurements on three samples, for which the heat treatment conditions are indicated as A, B and C in Fig. 5.

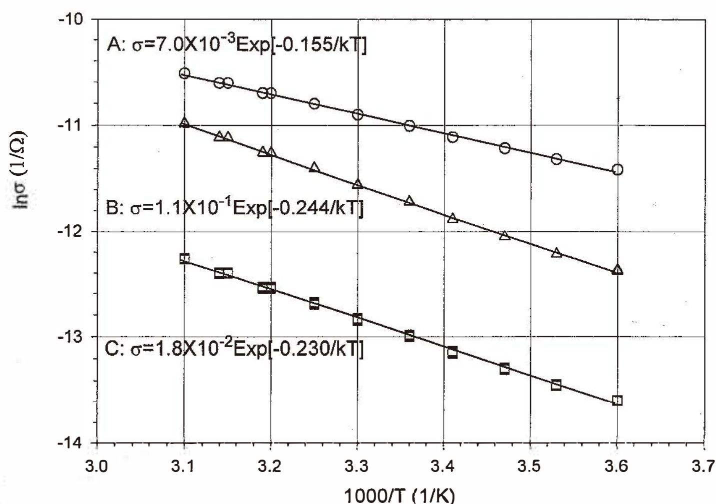

Fig. 6. The measured conductance of three samples with different annealing conditions. All show the Arrhenius behavior in the plot. Sample B provides the best TCR value.

The three samples were also chosen for noise measurement; the results are shown in Figs. 7(a), 7(b) and 7(c). It is obvious that sample B has the lowest flicker noise (1/f noise) of the three. The spectral density of the flicker noise fits very closely to the formula[7,8]

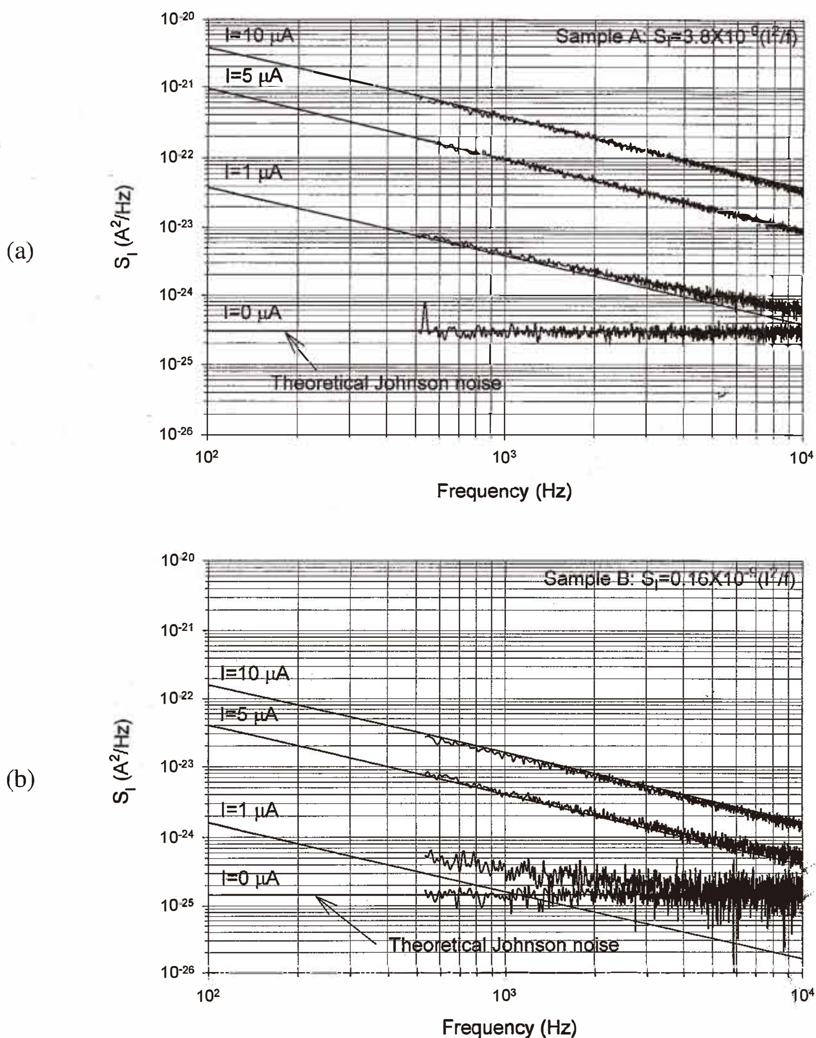

Fig. 7. The measured noise of samples A and B (Fig. 7(a) and 7(b)) as denoted in Fig. 5. Note that sample B has the lowest flicker noise.

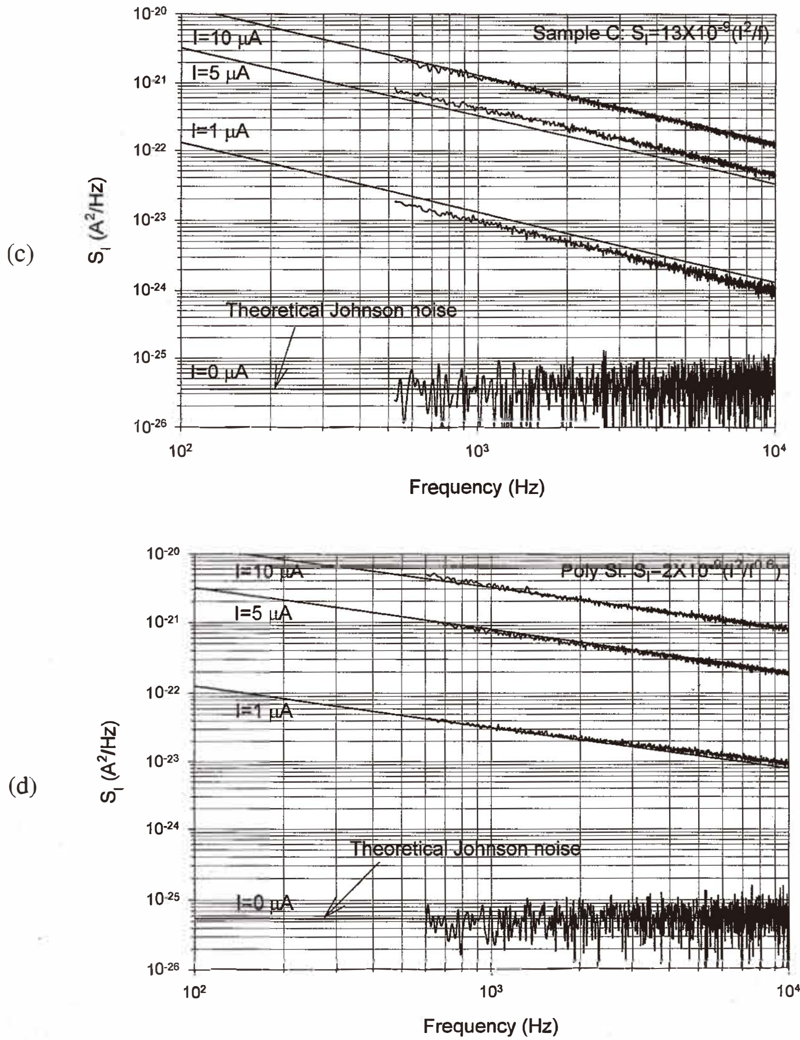

Fig. 7. The measured noise of sample C as denoted in Fig. 5. For comparison, Fig. 7(d) shows a polysilicon sensor made in a standard MOS foundry using a 1.2 μm rule with estimated doping of 2.6×10^{18} cm^{-3}; this has much higher flicker noise.

$$S_I = K\frac{I^2}{f}, \text{ (A}^2\text{/Hz)} \tag{1}$$

with K=3.8×10^{-9}, 0.16×10^{-9} and 13×10^{-9} for samples A, B and C, respectively.

For all sensors, low noise is as important for performance as high responsivity. From this viewpoint, sample B is the best choice among the three; therefore, it is used for further analysis. In Fig. 7(d), for purposes of comparison, we also show the noise measured in the polysilicon sensor fabricated in a CMOS foundry using a 1.2 μm feature. The flicker noise in the sensor is much larger than that in the Ge sensors illustrated here. This confirms our previous statement that, because polysilicon has higher energy gap, it is rich in undesirable deep-level traps in comparison with Ge, whose shallow trap levels generate smaller flicker noise. This is also the reason Ge was chosen as the sensor material in this study.

Sample B was further measured for responsivity, and the results are depicted in Fig. 8. In 1-atm air, the responsivity is slightly over 7 kV/W with a flat-band frequency up to 100 Hz. In a 10^{-3}-Torr vacuum, it climbs to nearly 400 kV/W at 1 Hz, which is ~52 times higher than the former. This indicates that gaseous thermal conduction is the dominating mechanism of heat-loss in this sensor structure. The detailed theory has been interpreted clearly by us in previous articles,[16–18] and all the thermal parameters of the device can be extracted according to the theory[19] as applied in this study. The flat-band responsivity varies with the vacuum pressure in the chamber as shown in Fig. 9. It indicates that a pressure as low as 10^{-2} Torr is enough to reach the responsivity limit of the microbolometer. This pressure, which is much lower than that reported by Kudoh *et al.*,[20] requires no delicate ultra-high-vacuum package technique.

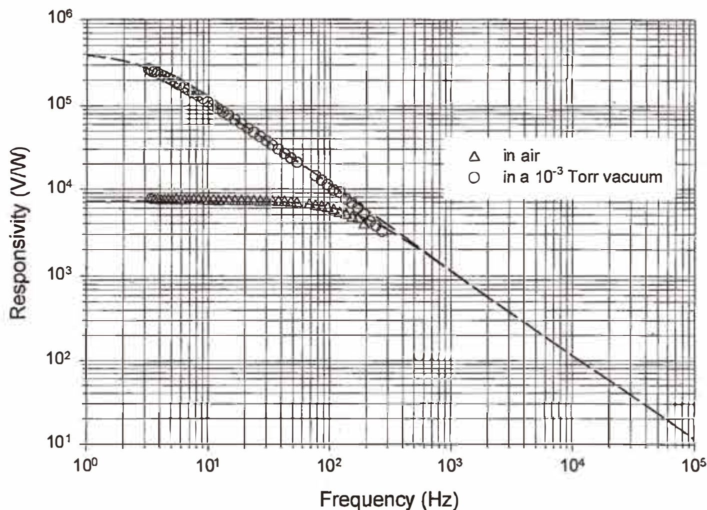

Fig. 8. The responsivity of sample B measured in vacuum and in 1-atm air.

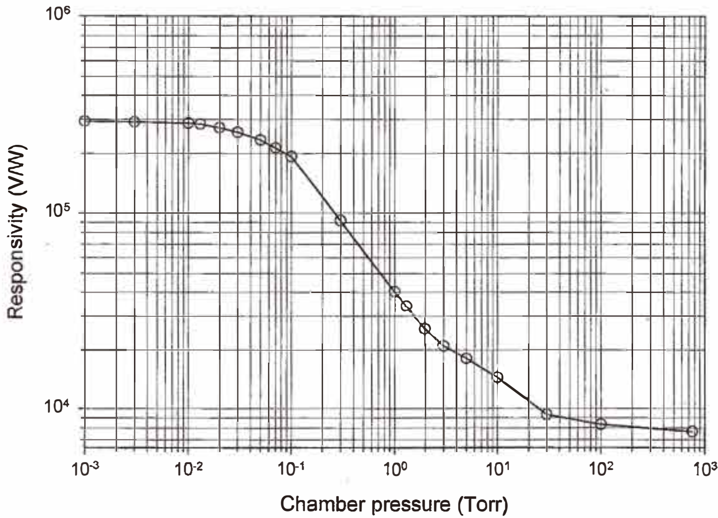

Fig. 9. The responsivity of sample B as the function of the vacuum chamber pressure, which shows that gaseous thermal conductivity is the dominant heat loss mechanism of the device in 1-atm air.

One also should note that the product of responsivity and bandwidth of a bolometer is a constant function of ε/H,[16] the ratio of the emissivity to the thermal capacitance; therefore, any desired bandwidth for a special application can be tuned by setting a proper pressure in the package.

According to the above data, the noise equivalent power (NEP) and the normalized detectivity (D*) of the sensor can be calculated; these values are depicted in Fig. 10. In a vacuum, D* can be as high as 1.2×10^8 cmHz$^{1/2}$/W at 3 Hz. This value and its speed, in comparison with current thermopile and pyroelectric products, are very suitable for a radiation detector for commercial tympanic thermometers.[21] One notes that the voltage responsivity is

$$R_V = \frac{\varepsilon\alpha V}{G}, \text{ (V/W)} \tag{2}$$

and the flicker noise voltage according to eq. (1) is

$$\upsilon_n = \sqrt{\frac{K}{f}} \cdot V, \text{ (V / }\sqrt{\text{Hz}}\text{)} \tag{3}$$

Here, for the case of dominant flicker noise, the bolometer NEP becomes

$$NEP = \frac{\upsilon_n}{R_V} = \sqrt{\frac{K}{f}} \cdot \frac{G}{\varepsilon\alpha}, \text{ (V / }\sqrt{\text{Hz}}\text{)} \tag{4}$$

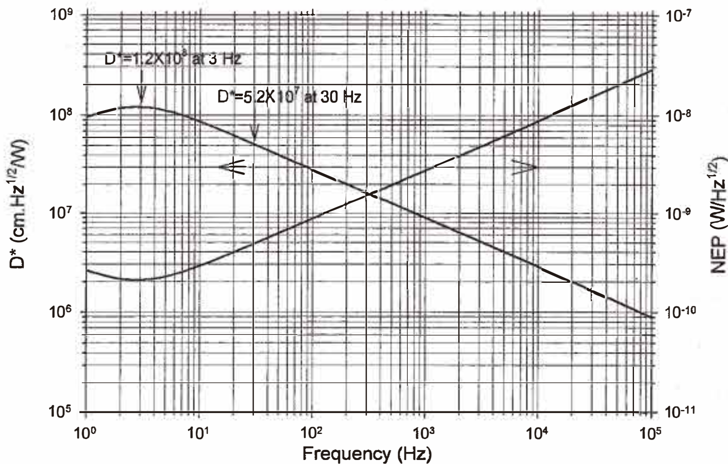

Fig. 10. The calculated normalized detectivity and noise equipment power of sample B. The D* is as high as 1.2×10^8 at 3 Hz, and the NEP is 0.2 nW/Hz$^{1/2}$, which is about 2.5 times lower than the required performance of a tympanic detector.

which is independent of the bias current.

In high vacuum, the thermal conductance of the device is dominated by the lead solid conductance, which is evaluated to be 7×10^{-7} W/°C for the fabricated devices. Since the best performance in the reported articles is 1×10^{-7} W/°C ,[4,5] it is expected that a Ge sensor treated as sample B can be further improved in responsivity if a smaller geometry is adopted.

Since the titanium thin film has strong tendency to oxidize, we suspect that the large 1/f noise arises from the interface between the Ge sensor and the titanium electrodes, where a non-ohmic contact might exist. Hence, reducing the noise by improving the contact quality is worth further study.

All the processes, thermal and electrical parameters of the three samples are included in Table 1 for reference.

4. Conclusions

The Ge thin-film bolometer under proper annealing conditions exhibits high sensitivity which qualifies it for use in commercial tympanic thermometers. The process steps are compatible with current CMOS fabrication, which allows monolithic integration of CMOS devices; hence, low-cost manufacturing can be achieved.

Table 1.
Summary of the three fabricated Ge microbolometers.

Ge sample	A	B	C
Annealing temperature (°C)	350	370	460
Annealing time (h)	2	2	2
Resistance (kΩ)	57	115	405
Resistivity (kΩ-cm)	13	26	92
B value (K)	1799	2824	2668
TCR (%/°C)	–2.00	–3.14	–2.96
Activation energy (eV)	0.155	0.244	0.233
Thermal conductance G in air (μW/K)*	28	28	28
Thermal conductance G in vacuum (μW/K)*	0.54	0.54	0.54
Calculated radiation-limited G (μW/K)*	0.57	0.57	0.57
Thermal capacitance H (10^{-8} J/K)	2.8	2.8	2.8
Thermal time constant in air (ms)*	1	1	1
Thermal time constant in vacuum (ms)*	52	52	52
Johnson noise (nV/$Hz^{1/2}$)	30	43	80
1/f noise constant K (10^{-9})	3.8	0.16	13
D* at 3 Hz in vacuum (10^8 cm$Hz^{1/2}$/W)*		1.2	
NEP at 3 Hz (nW/$Hz^{1/2}$)*		0.2	

*: Assumed emissivity $\varepsilon = 0.8$

Acknowledgement

The authors are indebted to Professor Kuan of National Taiwan University for assisting in the noise measurements. They wish to express their appreciation to the Semiconductor Research Center of NCTU for the sample preparation. This project is supported by the National Science Council of Taiwan under project contract No. NSC88-2218-E009-013.

References

1 N. T. Langley: Proc. Am. Acad. Arts Sci. **16** (1881) 342.
2 H. Baltes and O. Paul: Thermal Sensors Fabricated by CMOS and Micromachining, Sensors and Materials **8** (1996) 409.
3 N. Fujitsuka, J. Sakata, Y. Miyachi, K. Mizuno, K. Ohtsuka and Y. Taga: Monolithic Pyroelectric Infrared Image Sensor Using PVDF Thin Film, Transducers '97 2 (1997) 4B3 02.
4 R. A. Wood: Uncooled Thermal Imaging with Monolithic Silicon Focal Planes, SPIE 2020 (1993) 322.
5 A. Tanaka, S. Matsumoto, N. Tsukamoto, S. Itoh, K. Chiba, T. Endoh, A. Nakazato, K. Okuyama, Y. Kumazawa, M. Hijikawa, H. Gotoh, T. Tanaka and N. Teranishi: Infrared Focal Plane Array Incorporating Silicon IC Process Compatible Bolometer, IEEE Trans. Electron Devices **43** (1996) 1844.
6 M. S. Liu, J. S. Haviland and C. J. Yue: Integrated Infrared Sensitive Bolometers, U.S. Patent No. 5260225 (1993).

7 H. C. de Graaff and M. T. M. Huybers: 1/f Noise in Polycrystalline Silicon Resistors, J. Appl. Phys. **54** (1983) 2504.
8 M. Y. Luo and G. Bosman: An Analytical Model for 1/f Noise in Polycrystalline Silicon Thin Films, IEEE Trans. Electron Devices **37** (1990) 768.
9 S. Sedky, P. Fiorini, M. Caymax, A. Verbist and C. Baert: Thermally Insulated Structures for IR Bolometers Made of Polycrystalline Silicon Germanium Alloys, Transducers '97 (1997) 1D3 10P.
10 E. Iborra, A. Sanz-Hervas and T. Rodriguez: High Sensitivity Bolometers Development, Rev. Sci. Instrum. **63** (1992) 4708.
11 F. J. Low: Low-Temperature Germanium Bolometer, Journal of Optical Society of America **51** (1961) 1300.
12 T. Mori, T. Kudoh, K. Komatsu and M. Kimura: Vacuum-Encapsulated Thermistor Bolometer Type Miniature Infrared Sensor, IEEE Proc. MEMS 3 (1994) 257.
13 B. C. S. Chou, J. S. Shie and C. N. Chen: Fabrication of Low-stress Dielectric Thin Film for Microsensor Applications, IEEE Electron Device Letters **18** (1997) 599.
14 F. Volklein: Thermal Conductivity and Diffusivity of a Thin Film SiO2-Si3N4 Sandwich System, Thin Solid Films **188** (1990) 27.
15 K. P. Chik and P. K. Lim: Annealing and Crystallization of Amorphous Germanium Thin Films, Thin Solid Films **35** (1976) 45.
16 J. S. Shie, Y. M. Chen, M. Ou-Yang and B. C. S. Chou: Characterization and Modeling of Metal-Film Microbolometer, IEEE J. Microelectromechanical Sys. **5** (1996) 298.
17 J. S. Shie, Y. M Chen and C. S. Sheen: Analysis of Optimal Bolometer Sensitivity with Linear Approximation, SPIE 2746 (1996) 113.
18 M. Ou-Yang, C. S. Sheen and J. S. Shie; Parameter Extraction of Resistive Thermal Microsensors by AC Electrical Method, IEEE Trans. Instrumentation and Measurement **47** (1998) 403.
19 Y. M. Chen, J. S. Shie and T. Hwang: Parameter Extraction of Resistive Thermal Sensors, Sensors and Actuators A **55** (1996) 43.
20 T. Kudoh, S. I. Ikebe, H. Satow, K. Komatsu and M. Kimura: A Highly Sensitivity Thermistor Bolometer for a Clinical Tympanic Thermometer, Sensors and Actuators A **55** (1996) 13.
21 M. Ou-Yang, J. S. Shie and C. Tsao: Design and Analysis of Electrically Calibrated Tympanic Thermometers, Applied Optics **37** (1998) 2708.